Heliyon 6 (2020) e04671

Contents lists available at ScienceDirect

Heliyon

journal homepage: www.cell.com/heliyon

Research article

Antibacterial and cytotoxic activities of new sphingolipids and other constituents isolated from *Cissus incisa* leaves☆

Deyani Nocedo-Mena [a,b,*], Verónica M. Rivas-Galindo [c], Patricia Navarro [d], Elvira Garza-González [e], Leticia González-Maya [f], María Yolanda Ríos [g], Abraham García [a], Francisco G. Ávalos-Alanís [a], José Rodríguez-Rodríguez [h], María del Rayo Camacho-Corona [a,**]

[a] *Universidad Autónoma de Nuevo León, Facultad de Ciencias Químicas. Av. Universidad S/N, Ciudad Universitaria, 66451, San Nicolás de los Garza, Nuevo León, Mexico*
[b] *Department of Organic Chemistry II, University of the Basque Country UPV/EHU, 48940, Leioa, Spain*
[c] *Universidad Autónoma de Nuevo León, Facultad de Medicina. Av. Gonzalitos and Madero S/N, Colonia Mitras Centro, 64460, Monterrey, Nuevo León, Mexico*
[d] *General Research Services, University of the Basque Country UPV/EHU, 48940, Leioa, Spain*
[e] *Universidad Autónoma de Nuevo León, Servicio de Gastroenterología, Hospital Universitario "Dr. José Eleuterio González". Av. Gonzalitos and Madero S/N, Colonia Mitras Centro, 64460, Monterrey, Nuevo León, Mexico*
[f] *Universidad Autónoma del Estado de Morelos, Facultad de Farmacia. Av. Universidad 1001, 62209, Cuernavaca, Morelos, Mexico*
[g] *Universidad Autónoma del Estado de Morelos, Centro de Investigaciones Químicas, IICBA. Av. Universidad 1001, 62209, Cuernavaca, Morelos, Mexico*
[h] *Instituto Tecnológico y de Estudios Superiores de Monterrey. Av. Eugenio Garza Sada Sur, Tecnológico, 64849, Monterrey, Nuevo León, Mexico*

ARTICLE INFO

Keywords:
Natural product chemistry
Cissus incisa
Traditional medicine
Sphingolipids
Antibacterial activity
Cytotoxic activity

ABSTRACT

Cissus incisa is used in traditional Mexican medicine to treat certain ailments, infectious or cancerous diseases. Excepting for our previous research, this species had no scientific reports validating its traditional use. In this study, we evaluated the antibacterial and cytotoxic properties of the sphingolipids and others phytocompounds isolated from *C. incisa* leaves to increase the scientific knowledge of the Mexican flora. The antibacterial activity was evaluated against Gram-positive and Gram-negative bacteria by the Microdilution method. Meanwhile, the cytotoxic potential was determined on six human cancer cells: PC3, Hep3B, HepG2, MCF7, A549, and HeLa; using an aqueous solution cell proliferation assay kit. A cell line of immortalized human hepatocytes (IHH) was included as a control of non-cancerous cells. Selectivity index (SI) was determined only against the hepatocellular carcinoma cell lines. The phytochemical investigation of *C. incisa* leaves resulted in the isolation and characterization of five compounds: 2-(2′-hydroxydecanoyl amino)-1,3,4-hexadecanotriol-8-ene **(1)**, 2,3-dihydroxypropyl tetracosanoate **(2)**, *β*-sitosterol-D-glucopyranoside **(3)**, *α*-amyrin-3-*O*-*β*-D-glucopyranoside **(4)**, and a mixture of cerebrosides **(5)**. Until now, this is the first report of the sphingolipids **(1)**, **(5-IV)** and **(5-V)**. Only the compound **(4)** and cerebrosides **(5)** exhibited antibacterial activity reaching a MIC value of 100 μg/mL against *Pseudomonas aeruginosa* resistant to carbapenems. While, the acetylated derivate of **(3)**, compound **(3Ac)** showed the best cytotoxic result against PC3 (IC_{50} = 43 ± 4 μg/mL) and Hep3B (IC_{50} = 49.0 ± 4 μg/mL) cancer cell lines. Likewise, **(3Ac)** achieved better SI values on HepG2 and Hep3B cell lines. This research reveals the importance of study medicinal plants, to identify bioactive molecules as sources of potential drugs. The presence of these compounds allows us to justify the use of this plant in traditional Mexican medicine.

☆ Linked article: Spectral data of new sphingolipids and other phytocompounds isolated from *Cissus incisa* leaves, Spectral data of new sphingolipids and other phytocompounds isolated from *Cissus incisa* leaves, Data in Brief, In Press.

* Corresponding author.
** Corresponding author.x
E-mail addresses: deyaninocedo@gmail.com (D. Nocedo-Mena), maria.camachocn@uanl.edu.mx (M.R. Camacho-Corona).

https://doi.org/10.1016/j.heliyon.2020.e04671
Received 6 May 2020; Received in revised form 10 July 2020; Accepted 5 August 2020

1. Introduction

The spread of antibiotic-resistant bacteria represents a substantial threat to morbidity and mortality worldwide. Multidrug-resistant infections are being considered by World Health Organization (WHO) as a global priority to develop new drugs (Tacconelli et al., 2018). Cancer constitutes another serious problem of public health in the world. It is a dangerous disease-causing high mortality among the human population. Historically, plants have provided a good source of anti-infective and anti-cancer agents. Some active ingredients in these medicines have been isolated from plants used by various cultures for the treatment of diseases with cancerous symptoms and the treatment of infections. For this reason, ethnomedical reports are considered of great value in drug discovery (Vega-Ávila et al., 2006; Rossiter et al., 2017; Gezici and Şekeroğlu, 2019).

The genus *Cissus*, which belongs to the Vitaceae family, comprises about 350 species of all continents. Many cultures have used locally available species belonging to this genus to treat several medical problems (Fernandes and Banu, 2012). Previous investigations point to antimicrobial and anticancer properties of some *Cissus* extracts: *C. quadrangularis* (whole plant) (Ndhlovu and Masika, 2017), *C. cornifolia* (leaves and roots) (Chipiti et al., 2017), *C. quadrangularis* (aerial parts) (Kumar et al., 2017), *C. quadrangularis* (stems) (Fouche et al., 2016).

Cissus incisa (Nutt.) Des Moul. ex S. Watson, commonly known as "hierba del buey" is a plant native to the southern United States and adjacent parts of northern Mexico. It is fast-growing, climbing, with attractive green toothed leaves. Its flowers are white in summer, giving rise to blackish fruits in autumn (Learn2Grow, 2016; SEINet, 2019). According to traditional Mexican medicine, its leaves are used to treat skin infections, abscesses, and tumors (Alvarado Vázquez et al., 2010). Excepting for our investigation, this species had no scientific reports and its traditional use was not validating.

Currently, many researchers are interested in giving scientific authentication and explanation to the biological activities of plants used in traditional medicine throughout the world. Traditional uses of *C. incisa* motivated our effort to investigate their phytochemistry and their pharmacological activities. Formerly, we have determined the antimicrobial properties of the chloroform/methanol, and hexane extracts of *C. incisa* leaves (Nocedo-Mena et al., 2020) and some active phytocompounds, including new antibacterial ceramides (Nocedo-Mena et al., Unpublished results). Ceramides and cerebrosides are sphingolipids that represent a significant proportion of the lipids in higher plants. Some studies suggest that they constitute up to 10 % of plant lipids. Novel plant lipid structures are still being discovered, and over two hundred have been identified in various species to date. The wide range of sphingolipid structures facilitates their function in a variety of cellular processes. This enables these molecules to be involved in diverse activities as the structural integrity of the membranes, membrane domain formation, and the response of plants to hypoxia and pathogen attack (Michaelson et al., 2016).

The present study aimed to determine the antibacterial and cytotoxic properties of the sphingolipids and other phytocompounds. Five natural products were isolated and characterized: 2-(2′-hydroxydecanoyl amino)-1,3,4-hexadecanotriol-8-ene **(1)**, 2,3-dihydroxypropyl tetracosanoate **(2)**, β-sitosterol-D-glucopyranoside **(3)**, α-amyrin-3-*O*-β-D-glucopyranoside **(4)** and a mixture of cerebrosides **(5)**. This is the first report of the sphingolipids **(1)**, **(5-IV)** and **(5-V)**. The structural elucidation was performed by a combination of spectroscopic analyses, including 1D and 2D NMR, UHPLC-QToF-MS and chemical reactions. Additionally, acetylated derivatives of the natural compounds were obtained.

The antibacterial potential of sphingolipids and the other compounds was evaluated, also their cytotoxic properties. Only **(4)** and **(5)** exhibited antibacterial activity with MIC values of 100 μg/mL each, against *P. aeruginosa* resistant to carbapenems. While, the β-sitosteryl β-D-tetraacetyl glucopyranoside **(3Ac)** showed the best cytotoxic result against PC3 ($IC_{50} = 43 \pm 4$ μg/mL) and Hep3B ($IC_{50} = 49.0 \pm 4$ μg/mL) cancer cell lines. Values obtained for Selectivity Index (SI) on hepatocellular carcinoma lines, revealed potentialities of the compounds for being used selectively to treat this type of cancer.

2. Materials and methods

2.1. General experimental procedures

Melting points were measured with a Thermo Scientific P12144Q Fisher-Johns Melting Point apparatus. Column chromatography (CC) was conducted with silica gel (EMD Chemicals Inc. brand, Sigma Aldrich). Thin-Layer Chromatography (TLC) was carried out on 0.2 mm thick silica gel plates (Merck 60 F254). Solvent systems used in TLC were: $CHCl_3$/MeOH, Hex/EtOAc, $CHCl_3$/Acetone, $CHCl_3$/MeOH/CH_3COOH. The chemicals and reagents were acquired from Sigma-Aldrich (St. Louis, Missouri, USA) or Baker (Baker, Phillipsburg, New Jersey, USA). Spots were detected by TLC using UV lamp (Spectroline brand) and solutions of ceric sulfate in sulfuric acid with subsequent heating. IR spectra were recorded with a Bruker ALPHA ATR-FTIR spectrometer. NMR spectra were obtained on a Bruker NMR 400 spectrometer operated at 400 MHz (^1H) and 100 MHz (^{13}C) using deuterated solvents with tetramethylsilane (TMS) as internal reference.

2.1.1. GC-MS analysis

Samples were processed on an Agilent Model 6890 Gas Chromatograph (Agilent Technologies, Santa Clara, CA, USA) with a Selective Mass Detector (Agilent Model 5973N) operated in the electronic impact mode at 70 eV. The technique was developed with the following conditions: column HP-5MS (30 m × 0.250 mm X 0.25 μm), the carrier gas was helium (1 mL/min constant flow), the initial oven temperature was 50 °C, rising 2 °C/min to 285 °C for 35 min (final time). The retention index of compounds was recorded with standard n-hydrocarbon calibration mixture (C10–C40, Honeywell Fluka, Germany) using 2.64 AMDIS software. The results were given with reference to the NIST library database version 1.7[a].

2.1.2. UHPLC-QToF-MS analysis

Ultra-High Performance Liquid Chromatography (UHPLC) was carried out using a Waters ACQUITY UPLC™ system (Milford, MA, USA). A reverse phase column (Acquity UPLC C18 CSH, 100 × 2.1 mm, 1.7 μm) and a pre-column (Acquity UPLC C18 CSH 1.7 μm VanGuardTM) were used at 65 °C. The samples were dissolved in $CHCl_3$/MeOH (1:2, v/v) at 25 μg/mL. Mobile phases consisted of acetonitrile and water (40:60, v/v) with 10 mM ammonium formate and 0.1% formic acid (phase A), and acetonitrile and isopropanol (10:90, v/v) with 10 mM ammonium formate and 0.1% formic acid (phase B). Flow rate was 500 μL/min and injection volume was 7.5 μL. The gradient used for the lipid profiling was established as follows: initial conditions were 40 % B, raised to 43 % B over 2.0 min and to 50 % B over 0.10 min more. During the next 9.90 min it was raised to 54 % B and in 0.1 min more to 70 % B. In 5.90 min, it was raised to 100 % B and held at 100 % B until 19.0 min, decreased to 40 % B over the next 0.1 min, and held at 40 % B 1.90 min for re-equilibration of the system prior to the next injection.

All mass spectrometry data was acquired on a SYNAPT G2 HDMS, with a quadrupole time of flight (Q-ToF) configuration (Waters, Milford, MA, USA), equipped with an Electrospray Ionization source (ESI) operated in positive mode. The capillary voltage was set to 1 kV. Nitrogen was used as desolvation and cone gas, at flow rates of 1000 L/h and 10 L/h, respectively. The source temperature was 120 °C and the desolvation temperature was 500 °C. A leucine-enkephalin solution (2 ng/μL) was used for lock-mass correction. The reference internal standard was introduced into the lock mass sprayer at a constant flow rate of 10 μL/min with an external pump. Data acquisition took place over the mass range 50–1200 u in resolution mode (FWHM≈20.000) with a scan time of 0.3 s and an inter-scan delay of 0.024 s. The cone voltage was set to 40 V. The mass spectrometer was operated in the continuum MS^E acquisition mode.

2.2. Vegetal material

Leaves from *C. incisa* were collected in Rayones, Nuevo León, México (Latitude: 25.0167°, Longitude: -100.05°, Altitude: 900 m), in October 2016. The identification was made by the biologist Mauricio Gonzalez Ferrara. The collected species was deposited in the herbarium of the Faculty of Biology of the Universidad Autónoma de Nuevo León under the register number 027499.

2.3. Extraction and isolation

The leaves were dried at room temperature for 2 weeks, milled in a knife mill until obtaining 809 g of dried and grounded plant material. The powder was extracted four times with $CHCl_3$/MeOH 1:1 (7 L) at room temperature and then filtered. The filtrate was concentrated under vacuum to afford the crude $CHCl_3$/MeOH extract (84 g), subjected to successive CCs, eluted with Hex/EtOAc/MeOH gradients until twenty-four pooled fractions (fr. A to fr. X) were obtained. Fr. E (Hex/EtOAc 85:15; 4 g) was analyzed by CC with Hex/EtOAc gradients until obtained 73 sub-fractions. Sub-fraction 37–46 (Hex/EtOAc 80:20; 16.2 mg) was then purified by another CC (Hex/CH_2Cl_2/Acetone) getting 138 sub-fractions. From this last CC, sub-fraction 121–126 (CH_2Cl_2/Acetone 96:4) yielded 12.1 mg (0.0015%) of a white solid **(1)**. Fr. O (Hex/EtOAc 70:30; 1.1 g) was subjected to a silica gel CC using CH_2Cl_2/EtOAc gradient, giving 110 sub-fractions. From sub-fraction 61–75 (CH_2Cl_2/EtOAc 80:20) precipitated a solid. This solid was purified by several re-crystallizations with CH_2Cl_2/EtOAc 80:20 until 18.9 mg (0.0023%) of a white solid **(2)** was obtained. Fr. T (EtOAc/MeOH 90:10; 2.78 g) was chromatographed using $CHCl_3$/MeOH gradient until 72 sub-fractions were acquired. From these, the sub-fraction 19–27 (solid, 4.12 g, $CHCl_3$/MeOH 80:20) was purified on a silica gel CC with $CHCl_3$/MeOH gradient, giving 102 sub-fractions. A yellowish-white solid precipitated from sub-fraction 79–90 ($CHCl_3$/MeOH 82:18), which was repeatedly washed with acetone, yielding 82 mg (0.01%) of a white solid **(3)**. Meanwhile, from sub-fraction 28–47 ($CHCl_3$/MeOH 80:20; 35.9 mg) a solid was obtained. It was washed with acetone and purified by recrystallization with chloroform obtaining 32.7 mg (0.004%) of the compound **(4)**. Fr. S and fr. U were joined because of chromatographic similarity giving 3.685 g of the mixture, which was subjected to CC using CH_2Cl_2/MeOH gradient until obtained 114 sub-fractions. From the sub-fractions 90–99 (CH_2Cl_2/MeOH 80:20) was obtained a precipitated, which was repeatedly washed with acetone, yielding 294 mg (0.036%) of a brown solid **(5)**. The purity of the natural products obtained was determined by the following criteria: chromatographic homogeneity, melting points and two-dimensional chromatography.

2-(2′-hydroxydecanoyl amino)-1,3,4-hexadecanotriol-8-ene ***(1)***. White solid, mp:123–125 °C, HRMS-ESI (positive ionization mode) *m/z*: 475.3250 $[M + H_2O]^+$, 457.3250 $[M]^+$ ($C_{26}H_{51}NO_5$, calc. 457.3767). ^{1}H NMR (400 MHz, $CDCl_3$) δ (ppm): 0.90 (t, J = 6.66 Hz, 6H, CH_3), 1.28 (brs, 22H, CH_2), 1.62 (m, 6H, CH_2), 1.99 (m, 2H, H-10), 2.05 (m, 2H, H-7), 3.65 (m, 2H, H-3, H-4), 3.82 (m, 1H, H-1β), 3.97 (m, 3H, H-2′, H-1α), 4.17 (m, 4H, H-2, OH), 5.42 (m, 2H, H-8, H-9), 7.02 (m, 1H, NH). ^{13}C NMR (100 MHz, $CDCl_3$) δ (ppm): 14.13 (2CH_3), 22.70 (CH_2), 24.18 (CH_2), 24.96 (CH_2), 29.37 (2CH_2), 29.48 (CH_2), 29.72 (7CH_2), 31.92 (C7), 31.94 (C10), 35.04 (C3′), 54.82 (C2), 64.78 (C1), 69.95 (C2′), 71.63 (C4), 74.46 (C3), 129.10 (C9), 129.48 (C8), 176.71 (C1′).

Cerebrosides ***(5)***. Brown solid, mp: 190–192 °C, IR (KBr) ν_{max} cm^{-1}: 3260, 2980, 2875, 1625, 1540, 1490, 1400, 1100, 1080, 740. HRMS-ESI (positive ionization mode) *m/z*: 872.7200 $[M + H]^+$, 844.6866 $[M + H]^+$, 759.6281 $[M]^+$, 810.6047 $[M\text{-OH}]^+$, 884.6484 $[M + H]^+$. UHPLC-QToF-MS *m/z*: 871.7200 $[M]^+$ ($C_{50}H_{97}NO_{10}$, calc. 871.7112), 843.6866 $[M]^+$ ($C_{48}H_{93}NO_{10}$, calc. 843.6799), 759.6281 $[M]^+$ ($C_{42}H_{81}NO_{10}$, calc. 759.5860), 827.6047 $[M]^+$ ($C_{47}H_{89}NO_{10}$, calc. 827.6486), 883.6487 $[M]^+$ ($C_{51}H_{97}NO_{10}$, calc. 883.7112). ^{1}H NMR (400 MHz, DMSO-*d6*) δ (ppm): 0.86 (t, J = 6.62 Hz, CH_3), 1.24 (CH_2), 1.48 (m, H-3′), 1.50 (m, H-5), 1.96 (m, H-7, H-10), 2.93 (ddd, J = 8.28 Hz, J = 8.5 Hz, J = 12.10 Hz, H-2″), 3.33 (m, H-4), 3.09 (m, H-4″, H-5″, H-3″), 3.43 (m, H-6″β, H-3), 3.66 (m, H-6″α, H-1β), 3.83 (m, H-1α, H-2′), 4.10 (m, H-2), 4.14 (d, J = 7.84 Hz, H-1″), 4.36 (t, J = 6.46 Hz, OH), 4.54 (t, J = 5.5 Hz, OH), 4.79 (m, OH), 4.96 (m, OH), 5.32 (m, H-8, H-9), 5.60 (d, J = 5.12 Hz, OH), 7.55 (d, J = 9.4 Hz, N–H). ^{13}C NMR (100 MHz, DMSO-*d6*) δ (ppm): 14.41 (CH_3), 22.57 (CH_2), 24.85 (CH_2), 24.90 (CH_2), 26.10 (CH_2), 27.14 (C7), 27.43 (C10), 29.08 (CH_2), 29.17 (CH_2), 29.20 (CH_2), 29.46 (CH_2), 29.49 (CH_2), 29.54 (CH_2), 29.57 (CH_2), 29.66 (CH_2), 31.77 (CH_2), 32.52 (C5), 34.81 (C3′), 50.34 (C2), 61.51 (C6″), 69.42 (C1), 70.46 (C4″), 71.01 (C4), 71.39 (C2′), 73.92 (C2″),74.64 (C3), 76.97 (C5″), 77.36 (C3″), 103.96 (C1″), 129.84 (C9), 130.18 (C8), 174.25 (C1′).

2.4. Methanolysis of *(5)*

A mixture of 5.0 mL of 1N HCl, 15 mL of MeOH, and 15 mg of **(5)** was refluxed for 4 h (N_2 atmosphere) with magnetic stirring. Water was added to the mixture. Furthermore, the solution was extracted with hexane. After drying with anhydrous Na_2SO_4, the hexane extract was purified by silica gel column chromatography eluted with $CHCl_3$/Acetone (98:2) to afford **5a** (5.6 mg) (Figure 1). **5a** was further analyzed by GC-MS: Peak 1 (t_R 14.01 min, methyl 2-hydroxyoctadecanoate), EI-MS *m/z*: 314 $[M]^+$, 298, 281, 267, 255, 207, 74, 55, 43, 32; Peak 2 (t_R 15.18 min, methyl 2-hydroxytricos-9-enoate), EI-MS *m/z*: 382 $[M]^+$, 341 $[M - (CH_3)\text{–}(CH = CH)]^+$, 282 $[341\text{–}CH_3OCO]^+$, 57, 41, 32; Peak 3 (t_R 16.28 min, methyl 2-hydroxytetracosanoate), EI-MS *m/z*: 398 $[M]^+$, 355 $[M\text{–}(CH_3)\text{–}(CH_2)_2]^+$, 341 $[355\text{–} (CH_2)]^+$, 327 $[341\text{–}(OH)]^+$, 283 $[327\text{–}COO]^+$, 57, 43; Peak 4 (t_R 16.29 min, 2-methyl hydroxyhexacosanoate), EI-MS *m/z* 426 $[M]^+$, 268 $[M\text{–} (CH_3COO)\text{–}(CH_3)\text{–}(CH_2)_6]^+$, 250 $[M\text{–}OH]^+$, 82, 68, 55, 43; Peak 5 (t_R 16.797 min, methyl 2-hydroxyheptacos-9-enoate), EI-MS *m/z*: 438 $[M]^+$, 355 $[438\text{–}(CH_3)\text{–}(CH_2)_3\text{–}(CH = CH)]^+$, 341 $[355\text{–}(CH_2)]^+$, 326 $[341\text{–} (CH_3)]^+$, 281 $[326\text{–}COOH]^+$, 82, 57, 43.

The aqueous MeOH layer was neutralized with NH_4OH and extracted with EtOAc. The EtOAc extract was concentrated to dryness and further purified by a Sephadex LH-20 column eluted by $CHCl_3$/MeOH (1:1) to provide a Long-Chain Base (LCB) **5b** (2.5 mg). The aqueous MeOH layer was then concentrated to dryness and purified on silica gel column ($CHCl_3$/MeOH/H_2O, 7:3:0.5) to give 3.0 mg of the methyl glucopyranoside (**5c**) (Figure 1).

2.4.1. Acetylation of 5b

The mixture of acetic anhydride (Ac_2O) (0.7 mL), pyridine (0.3 mL), and **5b** (2.5 mg) was allowed to stand at room temperature for 24 h, then diluted with 10 mL of EtOAc and extracted with H_2O (3 × 10 mL). The organic phase was purified by a Sephadex LH-20 column ($CHCl_3$/MeOH 1:1) giving the acetylated derivate (1.5 mg), this was analyzed by UHPLC-QToF-MS. The chromatogram revealed a peak at t_R 0.369 min: *m/z* 442.2977 $[M + H]^+$. HRMS-ESI: *m/z* 441.2977 $[M]^+$ ($C_{24}H_{43}NO_6$ calc. 441.3090), which corresponds to acetylated LCB.

2.5. Acetylation of isolated natural compounds

The acetylation reactions followed the same scheme used previously to natural products (McCarthy et al., 2005). As consequence, it was synthetized the corresponding acetylated derivates for **(1)**, **(2)**, **(3)**, **(4)**, and **(5)**.

2-(2′-acetoxidecanoyl amino)-1,3,4-hexadecanotriacetat-8-ene ***(1Ac)***, colorless resin. ^{1}H NMR (400 MHz, $CDCl_3$) δ (ppm): 0.88 (t, J = 6.44 Hz, 6H, CH_3), 1.25 (brs, CH_2), 1.67 (m, 4H, H-5, H-6), 1.82 (m, 2H, H-3′), 1.95 (m, 2H, H-7), 2.03 (s, 3H, CH_3CO-1), 2.06 (s, 3H, CH_3CO-4), 2.09 (s, 3H, CH_3CO-3), 2.18 (s, 3H, CH_3CO-2′), 4.01 (dd, J = 11.72 Hz, 2.12 Hz, 1H, H-1β), 4.36 (dd, J = 11.52 Hz, 6.18 Hz, 1H, H-1α), 4.45 (m, 1H, H-2), 4.95 (d, J = 9.72 Hz, 1H, H-4), 5.10 (m, 2H, H- 2′, H-3), 5.37 (m, 2H, H-8, H-9), 6.60 (d, J = 9.04 Hz, 1H, NH). ^{13}C NMR (100 MHz, $CDCl_3$) δ (ppm): 14.13 (CH_3), 20.70 (CH_3CO-1), 20.76 (CH_3CO-4), 20.89 (CH_3CO-3), 21.04 (CH_3CO-2′), 22.71 (CH_2), 24.91 (CH_2), 25.53 (CH_2), 28.61 (C5), 29.25 (CH_2), 29.38 (CH_2), 29.45 (CH_2), 29.57 (CH_2), 29.60 (CH_2), 29.63

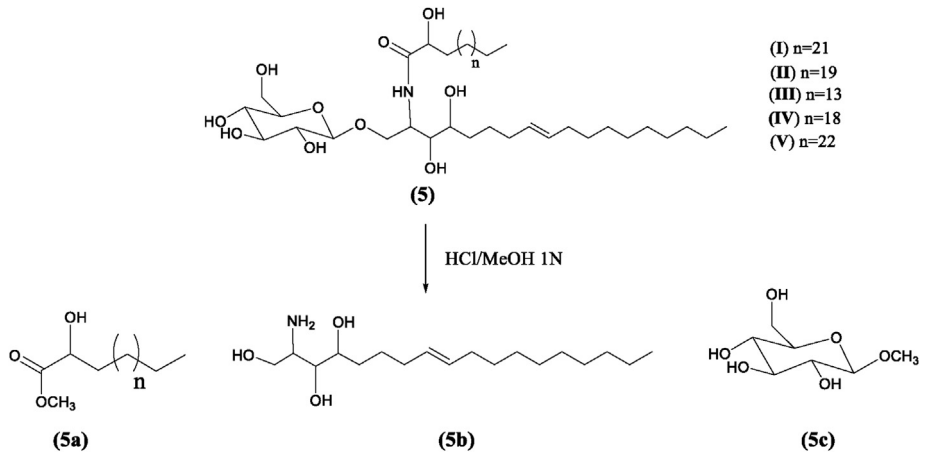

Figure 1. Scheme for the methanolysis of **(5)**.

(CH_2), 29.68 (CH_2), 29.73 (CH_2), 31.80 (CH_2), 31.94 (C3′), 32.21 (C10), 32.62 (C7), 47.86 (C2), 62.35 (C1), 72.30 (C-2′), 74.02 (C3), 72.70 (C4), 129.29 (C9), 131.20 (C8), 170.04 (C1′), 170.90 (CH_3CO- 4), 170.98 (CH_3CO-1), 171.31 (CH_3CO-2′, CH_3CO-3).

Acetylated cerebrosides ***(5Ac)***. ^{1}H NMR (400 MHz, $CDCl_3$) δ (ppm): 0.90 (t, $J = 6.62$ Hz, Me), 1.27 (brs, CH_2), 1.62 (m, H-10), 1.85 (m, H-3′, H-5), 1.97 (m, H-7), 2.01 (s, CH_3CO-4), 2.04 (s, CH_3CO-3), 2.06 (s, CH_3CO-6″, 4″), 2.08 (s, CH_3CO-3″), 2.11 (s, CH_3CO-2″), 2.25 (s, CH_3CO-2′), 3.71 (m, H-4″, H-6″β), 3.88 (d, $J = 9.8$ Hz, H-6″α), 4.14 (d, $J = 11.12$ Hz, H-1β), 4.27 (m, H-2, H-1α), 4.49 (d, $J = 8.0$ Hz, H-1″), 4.91 (m, H-4, H-2″), 5.15 (m, H-5″, H-3, H-2′, H-3″), 5.36 (m, H-8, H-9), 6.79 (d, $J = 8.76$ Hz, N–H). ^{13}C NMR (100 MHz, $CDCl_3$) δ (ppm): 14.13 (CH_3), 20.55 (CH_3CO-6″), 20.59 (CH_3CO-3″), 20.68 (CH_3CO-2″), 20.72 (CH_3CO-4″), 20.94 (CH_3CO-3), 21.01 (CH_3CO-4), 21.03 (CH_3CO-2′), 22.70 (CH_2), 24.90 (CH_2), 24.92 (CH_2), 25.75 (CH_2), 26.88 (CH_2), 27.29 (C10), 27.85, 27.95 (C17), 29.26 (CH_2) 29.29 (CH_2), 29.37 (CH_2), 29.49 (CH_2), 29.56 (CH_2), 29.62 (CH_2), 29.67 (CH_2), 29.72 (CH_2), 31.77 (CH_2), 31.92 (C5), 31.93 (C3′), 48.27 (C2), 61.76 (C1), 66.69 (C6″), 68.12 (C5″), 71.26 (C2′), 71.66 (C3″), 71.91 (C4″), 72.75 (C2″), 73.19 (C4), 73.98 (C3), 100.44 (C1″), 128.77 (C9), 130.68 (C8), 169.31(C1′), 169.39 (CH_3CO-3″), 169.80 (CH_3CO-2″), 169.98 (CH_3CO-6″), 170.23 (CH_3CO-4″), 170.31 (CH_3CO-4), 170.64 (CH_3CO-3), 171.11 (CH_3CO-2′).

2.6. Biological assays

For antibacterial activity, double-distilled water, dimethyl sulfoxide (DMSO) (JT Baker, USA), INC-80 incubator (Prendo), sterile 96-well round-bottom microplates with lid (Corning Costar, New York), and Mueller Hinton medium were used (Becton Dickinson). Strains of drug-resistant clinical isolates were obtained from the University Hospital Dr. Eleuterio González of the Universidad Autónoma de Nuevo León. Four of these bacteria are included in the list of priority pathogens issued by the WHO, 2017. For cytotoxic activity, the cell lines tested were obtained from ATCC (American Type Culture Collection, Manassas, VA, USA), RPMI-1640 medium (Sigma Aldrich, St. Louis, MO, USA), DMEM (Invitrogen, Thermo Fisher Scientific, Inc., Waltham, MA, USA) and fetal bovine serum (SFB, Invitrogen), Cell Titer 96® aqueous solution cell proliferation assay kit (Promega, Madison, WI, USA), automated ELISA reader.

2.6.1. Antibacterial activity

Gram-positive bacteria tested: Methicillin-Resistant *Staphylococcus aureus* (14–2095), Linezolid-resistant *Staphylococcus epidermidis* (14–583), Vancomycin-resistant *Enterococcus faecium* (10–984). Gram-negative bacteria: Carbapenems-resistant *Acinetobacter baumannii* (12–666), *Escherichia coli* producing extended-spectrum beta-lactamase (14–2081), *P. aeruginosa* resistant to carbapenems (13–1391), carbapenems-resistant *Klebsiella pneumoniae* NDM-1+ (14–3335), *Klebsiella pneumoniae* producer of ESBL (14–2081) and carbapenems-resistant *Klebsiella pneumoniae* (OXA-48 positive). Only compounds **(2)**, **(3)**, **(4)**, **(5)** and their acetylated derivates were tested, compound **(1)** was obtained in small quantity thus it was not tested. The antibacterial activity was developed by microdilution method previously reported by Zgoda and Porter (2001). The range of concentrations for the compounds was: 200, 100, 50, 25, 12.5, 6.25, and 3.12 μg/mL. Levofloxacin was used as positive control with the same concentrations, while DMSO (6%–0.09%, v/v) was the negative control. The Minimum Inhibitory Concentration (MIC) was determined as the Minimum Concentration of the compound that inhibits the growth of the bacteria. The experiments were repeated three times.

2.6.2. Cytotoxic activity

The compounds were evaluated for their cytotoxic activity in human cancer cells: PC3 (prostate), Hep3B and HepG2 (hepatocellular), MCF7 (breast), A549 (lung) and HeLa (cervical). In addition, a cell line of immortalized human hepatocytes (IHH) was included as a control of non-cancerous cells. PC3 cells were cultured in RPMI-1640 medium, while Hep3B, HepG2, IHH, MCF7, A549 and HeLa in DMEM and supplemented with fetal bovine serum 10% and with 2 mM glutamine. All cultures were incubated at 37 °C in a 5% CO_2 atmosphere (Basu et al., 2006). The amount of viable cells without proliferation was determined using the Cell Titer 96® proliferation kit, following the manufacturer's instructions (Promega, Madison, WI, USA). Cell viability was determined by absorbance at 450 nm using an automated ELISA reader. The concentrations used were 100, 10, 1, 0.1, and 0.01 μg/mL to obtain a dose/response curve. The experiments were performed in triplicate in three independent experiments. Paclitaxel was used as reference. The data were analyzed in the Prism 5.0 statistical program. IC_{50} values were determined by regression analysis.

Selectivity Index was determined only against the hepatocellular carcinoma lines. This allowed determining the selectivity of the cytotoxic activity in them. SI was calculated as followed (Badisa et al., 2009):

$$SI = \frac{IC_{50}\ IHH\ cell}{IC_{50}\ cancer\ cell}$$

3. Results

3.1. Structure elucidation

Phytochemical investigation of $CHCl_3$/MeOH extract of *C. incisa* resulted in the isolation of a new ceramide **(1)**, new cerebrosides within the genus **(5)**, of which **(5-IV)** and **(5-V)** are reported for the first time, and three known compounds: 2,3-dihydroxypropyl tetracosanoate **(2)** (Hernández-Galicia et al., 2007), β-sitosterol-D-glucopyranoside **(3)** (Njinga et al., 2016), and α-amyrin-3-*O*-β-D-glucopyranoside **(4)** (Kang

et al., 2011) (Figure 2). These compounds were identified by their spectroscopic data and by comparing with those reported above, as well that their acetylated derivates (Peshin and Kar, 2017).

2-(2′-hydroxydecanoyl amino)-1,3,4-hexadecanotriol-8-ene ***(1)*** was obtained as a white powder. The molecular formula of $C_{26}H_{51}NO_5$ was deduced from HRMS-ESI (positive ion mode) which showed the molecular ion peak at *m/z* 475.3250 $[M + H_2O]^+$. The ^1H and ^{13}C NMR spectra of **(1)** gave signals characteristics of two long chain aliphatic moieties consistent of methylenes (δ_H 1.28, brs, 22H; 1.62, m, 6H; δ_C 22.70–29.72) and two terminal methyls (δ_H 0.90, t, J = 6.66 Hz; δ_C 14.13) linked through a secondary amide linkage (δ_H 7.02, m; δ_C 176.71), proposing the structure of a natural ceramide. This was further supported by GC-MS analysis yielding a peak at t_R = 105.92 min, corresponding to *m/z* 405 $[M\text{-}3OH]^+$. The EI-MS spectra of **(1)** allowed to identify a LCB and a α-hydroxylated Long-Chain Fatty Acid (LCFA). The 1,3,4 trihydroxylated LCB was confirmed by the ion *m/z* 287 ($C_{16}H_{33}NO_3$), while the *m/z* 171 ($C_{10}H_{19}O_2$) corresponded to the LCFA (Figure 3). Additionally, ^1H NMR also revealed the presence of δ_H 5.42 olefinic protons attributable to a double bond, supported by two ethylenic carbons at δ_C 129.10 and δ_C 129.48. The position of the double bond was set at C8–C9 according to Michaelson et al. (2016) criteria. The confirmation was found in the EI-MS spectra by the fragments *m/z* 161 ($C_7H_{15}NO_3$) and 187 ($C_9H_{17}NO_3$) resulting from the rupture of the LCB on both sides of the double bond (Figure 3). The double bond was determined to be *trans*, according to the chemical shifts of the allyl carbons: δ_C 31.94 (C7) and δ_C 31.92 (C10). The chemical shifts of **(1)** were compared with the data already reported of natural sphingolipids (Tapondjou et al., 2005) and synthetic (Sugiyama et al., 1991), finding similarities that confirms **(1)** is a ceramide. The elucidation of the structural skeleton was completed based on the above comparison. Until our knowledge, there is no evidence in the literature of this ceramide, being this study the first report of its isolation and characterization.

The four hydroxyl groups of **(1)** were confirmed by means of acetylation and by the ^1H and ^{13}C NMR spectra of their corresponding tetraacetyl derivative: 2-(2′-acetoxidecanoyl amino)-1,3,4-hexadecanotriacetat-8-ene **(1Ac)**. Four singlets of acetyl groups were observed in δ_H (ppm): 2.03

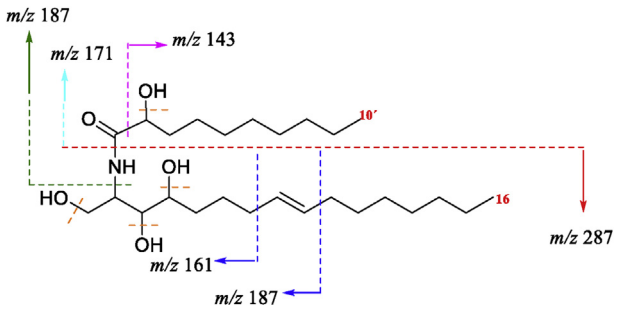

Figure 3. Fragmentation patterns of **(1)** that justify ions obtained in the EI-MS spectrum.

(CH_3CO-1), 2.06 (CH_3CO-4), 2.09 (CH_3CO-3), 2.18 (CH_3CO-2′). Four methyls attached to the ester carbonyl group in δ_C (ppm): 20.70 (CH_3CO-1), 20.76 (CH_3CO-4), 20.89 (CH_3CO-3), 21.04 (CH_3CO-2′), and four ester carbonyls in δ_C (ppm): 170.90 (CH_3CO- 4), 170.98 (CH_3CO-1), 171.31 (CH_3CO-2′, CH_3CO-3).

^1H NMR showed the signals indicative of ceramides: a high field signal corresponding to the terminal methyl (δ_H 0.88), then a broad signal corresponding to the long aliphatic chains (δ_H 1.25), a methine bound to nitrogen (δ_H 4.45). Finally, the proton of the secondary amide at 6.60 ppm (J = 9.04 Hz) supported by the signal of its carbonyl at 170.04 (C1′). Additionally, in the region between δ_H 4.0 and 5.1 ppm, appeared the geminal hydrogens to the ester groups (H-1β, H-1α, H-2′, H-3, H-4).

The double bond was located at position C-8 of the LCB because of biogenetic considerations (Michaelson et al., 2016) and is supported by the COSY correlation between H-7/H-8 (δ_H 1.95/δ_H 5.37) and HMBC correlation between H-7/C9 (δ_H 1.95/δ_C 129.29). The geometry of this bond was determined to be *trans*, according to the chemical shifts of the adjacent carbons. Being reported in the literature that (*E*) isomers appear around 32 ppm, while the (*Z*) at 27 ppm (Lü et al., 2008). The presence of a 1,3,4-triacetylated LCB was deduced from COSY data: δ_H 6.60 (NH), gave a crossed peak with the signal at δ_H 4.45 (H-2). Which, in turn,

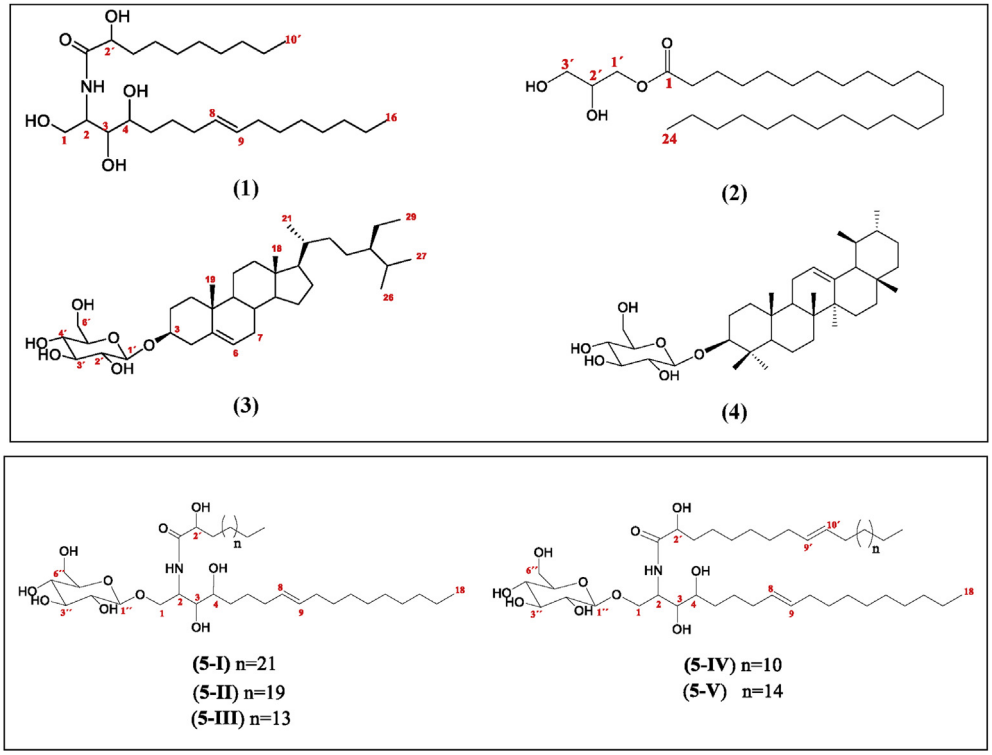

Figure 2. Chemical structures of **(1)** to **(5)**.

showed crossed peaks with methylene protons (H-1) at δ_H 4.36 and δ_H 4.01 and with H-3 (δ_H 5.10). The latter was correlated with the signal at δ_H 4.95 (H-4). Binding of LCB to fatty acid was confirmed by the HMBC correlation between H-1α and C1′ (δ_H 4.36 and δ_C 170.04) (Figure 4). The comparison of the chemical shifts of **(1Ac)** was similar to those of another previously described acetylated sphingolipid (Lin et al., 2004).

Cerebrosides ***(5)*** were analyzed by UHPLC-QToF-MS. The chromatogram showed a series of peaks at different t_R indicating the presence of a mixture of homologous compounds. The abundance percentages according to the chromatogram were: 30% (**5-I**, t_R 0.34 min); 8% (**5-II**, t_R 0.78 min); 46% (**5-III**, t_R 1.61 min); 10% (**5-IV**, t_R 4.21 min); and 6% (**5-V**, t_R 7.19 min). Thus, the HRMS-ESI (positive ionization mode) showed peaks at: *m/z* 872 $[M + H]^+$, 844 $[M + H]^+$, 759 $[M]^+$, 810 $[M\text{-OH}]^+$, and 883 $[M]^+$. The IR absorption band at 3260 cm^{-1} and 1080 cm^{-1} indicated the existence of hydroxyl and amide groups. The typical IR absorptions at 1625 cm^{-1} and 1540 cm^{-1} suggested **(5)** was a secondary amide derivative, which was supported by the presence of a nitrogen-attached proton at δ_H 7.55 (d, J = 9.4 Hz), a nitrogen-attached carbon at δ_C 50.34 and a carbonyl carbon at δ_C 174.25 in the ^1H and ^{13}C NMR spectra. Olefinic protons at δ_H 5.32 (H-8 and H-9) and olefinic carbons at δ_C 130.18 and 129.84 were attributable to a double bond. The ^1H spectra also showed the presence of multiple proton signals between δ_H 1.25–1.96 and a triplet proton signal at δ_H 0.86 (J = 6.62 Hz), suggesting the presence of long-aliphatic chains. A sugar moiety could be distinguished in the structure of **(5)**, which indicated by an anomeric proton signal at δ_H 4.14 and an anomeric carbon signal at δ_C 103.96 in the ^1H and ^{13}C spectra. A comparison of the spectroscopic data of **(5)** with those of cerebroside (Lü et al., 2008) indicated that **(5)** is a cerebroside analogue.

Methanolysis (Zhang et al., 2007) of **(5)** yielded a mixture of Fatty Acid Methyl Esters (FAME) (**5a**), a trihydroxy LCB (**5b**), and a methyl glucopyranoside (**5c**) (Figure 1). **5a** were identified by GC-MS as methyl 2-hydroxyoctadecanoate, methyl 2-hydroxytricos-9-enoate, methyl 2-hydroxytetracosanoate, 2-methyl hydroxyhexacosanoate, methyl 2-hydroxyheptacos-9-enoate. In order to establish the structure of the LCB, **5b** was acetylated with Ac_2O and pyridine. This was subjected to UHPLC-QToF-MS analysis. The HRMS-ESI spectra of the peak at t_R 0.369 min showed characteristic fragments at *m/z* 302, 178, 138 and 96 which indicated the structure of derivate should be 1,3, 4-triacetoxy-2-aminooctadec-8-ene.

The position of the double bond in the LCB was determined based on the biogenetic origin (Michaelson et al., 2016). The above is supported by the *m/z* 153 ion in HRMS-ESI spectra of **(5)**, and by the strong COSY correlation observed between protons H-7/H-10 (δ 1.96) with H-8/H-9 (δ 5.32). Similarly, the HMBC correlations between H-7/H-10 with C9/C8 confirmed this position in the LCB. The double bond was determined to be *Z* geometry by its adjacent carbon signals at δ 27.14 (C7) and 27.43 (C10) (Inagaki et al., 1998). These correlations are shown in Figure 4.

An anomeric proton at δ_H 4.14 and six oxygenated carbon atoms at δ_C 103.96, 73.92, 77.36, 70.46, 76.97, 61.51 supported the presence of a glucopyranoside. This was confirmed analyzing by HRMS-ESI (negative mode) the methylated glucose obtained from the methanolysis of **(5)**. The presence of *m/z* 194 $[M]^-$ fully justified the methylglucopyranoside. It is confirmed that the monosaccharide is glucose by the coupling constants $J_{4\text{-}5}$ = 8.64 Hz and $J_{4\text{-}3}$ = 9.04 Hz, evidencing the axial-axial coupling for H-4″. The β configuration was also corroborated by J = 7.84 Hz of the anomeric proton, consistent with the expected axial-axial coupling for the β-glucose anomer.

The linkage of the three parts of **(5)** was determined by the NOESY experiment (Figure 4). In this, the proton signal of the δ_H 7.55 amide was correlated with the protons H-2′ (δ_H 3.83) of the long-chain fatty acid part, as well as with H-1β (δ 3.66) and H-2 (δ 4.10) of the LCB. Furthermore, the correlation between the H-1α/1β signals (δ 3.83/δ 3.66) of the LCB and the anomeric proton signal at δ 4.14 was also observed. Therefore, **(5)** was determined as the mixture of five cerebrosides: 1-*O*-β-glucopyranosyl-2-(2′-hydroxyhexacosanoyl amino)-1,3,4-octadecanetriol-8-ene **(5-I)**; 1-*O*-β-glucopyranosyl-2-(2′-hydroxytetracosanoyl amino)-1,3,4-octadecanetriol-8-ene **(5-II)**; 1-*O*-β-glucopyranosyl-2-(2′-hydroxyoctadecanoyl amino)-1,3,4-octadecanetriol-8-ene **(5-III)**; 1-*O*-β-glucopyranosyl-2-(2′-hydroxytricos-9-enoyl amino)-1,3,4-octadecanetriol-8-ene **(5-IV)**; 1-*O*-β-glucopyranosyl-2-(2′-hydroxyheptacos-9-enoyl amino)-1,3,4-octadecanetriol-8-ene **(5-V)** (Figure 2). As far as we know, it is the first characterization of **(5-IV)** and **(5-V)** in the literature. Additionally, it is the first report of all these cerebrosides **(5)** within the genus *Cissus*.

The presence of four hydroxyl groups was confirmed by means of acetylation of **(5)**. The acetylated derivative **(5Ac)** was analyzed using 1D and 2D NMR techniques. As a result of acetylation reaction, the singlet corresponding to the seven acetyl appeared as new signals in ^1H NMR, at δ_H: 2.01 ($\underline{CH_3}CO$-4), 2.04 ($\underline{CH_3}CO$-3), 2.06 ($\underline{CH_3}CO$-6″, 4″), 2.08 ($\underline{CH_3}CO$-3″), 2.11 ($\underline{CH_3}CO$-2″), and 2.25 ($\underline{CH_3}CO$-2′). These signals are supported by their respective carbons in the ^{13}C spectra, δ_C: 20.55 (CH_3CO-6″), 20.59 (CH_3CO-3″), 20.68 (CH_3CO-2″), 20.72 (CH_3CO-4″), 20.94 (CH_3CO-3), 21.01 (CH_3CO-4), and 21.03 (CH_3CO-2′). Finally, the carbons corresponding to carbonyls of the esters were observed between δ_C 169.39 and 171.11. Above signals confirmed the presence of the seven hydroxyls in the natural product. The position of the double bond in the LCB was determined by HRMS-ESI in the natural product. Correlations between H-8 and H-9 with C10 and C7 respectively, were observed in the HMBC of the **(5Ac)**. The *cis* configuration of the double bond was evidenced in the natural product and also in its acetylated derivative by chemical shifts of the carbons neighboring the double bond [δ 27.95 (C7), δ 27.29 (C10)]. The comparison of spectroscopic data of **(5Ac)** with a similar sphingolipid derivative (Lin et al., 2004) allowed us to verify the assignments.

3.2. Antibacterial activity

The results for the antibacterial activity of the compounds and their acetylated derivates are shown in Table 1. Practically no antibacterial

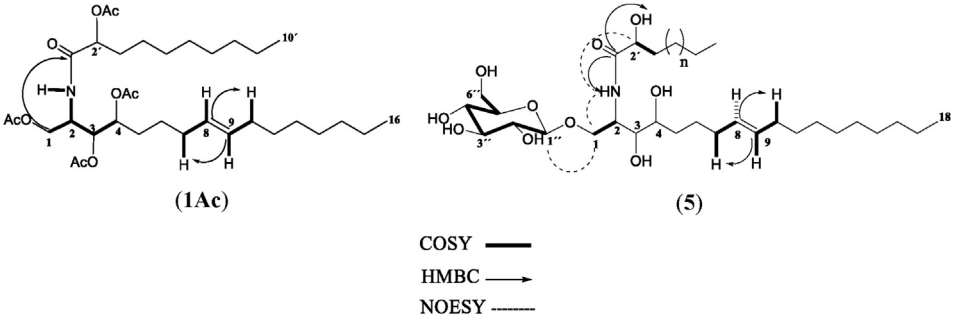

Figure 4. Key ^1H–^1H COSY, HMBC and NOESY correlations of **1Ac** and **5**.

Table 1. Antibacterial activity of selected compounds isolated from *C. incisa* leaves.

Compounds[a]	Strains of MDR bacteria[b]. MIC (μg/mL)								
	MRSA	LRSE	VREF	CRAB	ECPB	PARC	KPNDM-1+	KPPB	KPRO
(2)	>200	200	200	200	>200	200	200	>200	200
(2Ac)	>200	200	200	100	>200	200	200	>200	>200
(3)	>200	200	200	200	>200	200	>200	>200	200
(3Ac)	>200	>200	200	200	>200	200	>200	>200	200
(4)	>200	>200	>200	>200	>200	100	>200	>200	>200
(5)	>200	>200	>200	>200	>200	100	>200	>200	>200
(5Ac)	>200	>200	>200	200	>200	200	200	200	200
levofloxacin	12.5	6.25	12.5	12.5	12.5	12.5	>50	>50	>50

[a] 2,3-dihydroxypropyl tetracosanoate **(2);** 3-(tetracosanoyloxy) propane-1,2-diyl diacetate **(2Ac);** *β*-sitosterol-D-glucopyranoside **(3)**; *β*-sitosteryl *β*-D-tetraacetyl glucopyranoside **(3Ac)**; *α*-amyrin-3-O-*β*-D-glucopyranoside **(4)**; cerebrosides **(5)**; acetylated cerebrosides **(5Ac)**.

[b] (MRSA) Methicillin-Resistant *Staphylococcus aureus*); (LRSE) Linezolid-resistant *Staphylococcus epidermidis*; (VREF) Vancomycin-resistant *Enterococcus faecium*; (CRAB) Carbapenems-resistant *Acinetobacter baumannii*; (ECPB) *Escherichia coli* producing ESBL; (PARC) *Pseudomonas aeruginosa* resistant to carbapenems; (KPNDM-1+) carbapenems-resistant *Klebsiella pneumoniae* NDM-1+; (KPPB) *Klebsiella pneumoniae* producer of ESBL; (KPOX) carbapenems-resistant *Klebsiella pneumoniae* (OXA 48-positive).

activity was obtained against clinical isolates of MDR bacteria. Only **(4)** and **(5)** exhibited certain activity (MIC = 100 μg/mL) against *P. aeruginosa* resistant to carbapenems. According to literature, the antibacterial activity of *α*-amyrin glucoside in *P. aeruginosa* has not been reported yet, conversely to its aglycone *α*-amyrin which has shown MIC = 1000 μg/mL on a *Vernonia auriculifera* screening (Kiplimo et al., 2011).

On the other hand, a cerebroside isolated from *Spathodea campanulata* obtained MIC = 12.5 μg/mL against ATCC strains of *P. aeruginosa*, outperforming to our study carried out on MDR isolates (Mbosso et al., 2008). However, a cerebrosides mixture from *Euphorbia peplis* was inactive against ATCC strains of *E. coli* and *S. aureus* with MIC >160 μg/mL (Cateni et al., 2003), agreeing with the results obtained on same strains. In a previous work, our research group reported the antibacterial activity of the $CHCl_3$/MeOH extract from *C. incisa* leaves (Nocedo-Mena et al., 2020). Using the classification for the inhibitory activity for natural extracts (Ndhlovu and Masika, 2017), the $CHCl_3$/MeOH extract was consider as a "strong inhibitor" of the bacterial growth. The most sensitive strains were vancomycin-resistant *Enterococcus faecium*; carbapenems-resistant *Acinetobacter baumannii*; and *P. aeruginosa* resistant to carbapenems (MIC = 125 μg/mL for each one). Then, according to the results here obtained, we can conclude that both compounds **(4)** and **(5)** contribute to the antibacterial activity displayed in the corresponding extract.

Regarding to the MIC values of the semi-synthetic derivatives, they did not exceed to their natural products, except **(2Ac)** against *A. baumannii* resistant to carbapenems (MIC = 100 μg/mL). None of natural product or derived were able to exceed the MIC value of the positive control used.

3.3. Cytotoxic activity

According to the criteria of the National Cancer Institute of the USA, a compound is considered active if it has an $IC_{50} \leq 4$ μg/mL on tumor cells (Suffness and Pezzuto, 1990). According to the above, none of the compounds evaluated classified with good anticancer activity. However, *β*-sitosteryl *β*-D-tetraacetyl glucopyranoside **(3Ac)** was the most active having IC_{50} values = 43 ± 4 μg/mL against the PC3 cancer line and 49.0 ± 4 μg/mL against Hep3B (Table 2).

The cytotoxic activity of $CHCl_3$/MeOH extract in PC3 lines was previously determined by this research group (IC_{50} = 57 ± 4 μg/mL) (Nocedo-Mena et al., Unpublished information). Analyzing the experimental results obtained here, compound **(3)** practically no contributes to the anticancer activity within the extract. Similar results were shown in a previous study, in which El-Halawany et al. (2018) determined a non-cytotoxic effect of **(3)** in lung cancer A-549, prostate cancer PC3 and liver cancer HepG2 cells (IC_{50} > 100 μg/mL). However, in the current study, its tetraacetylated derivative **(3Ac)** obtained the best results. It is important to point out that, as far we know, there is no reported cytotoxic activity for compound **(3Ac)** in any of the cancer lines tested.

The American Association for Cancer Research has suggested conducting *in vitro* toxicity studies of a pharmacological regimen in the same type cells to the cancer lines under study (Wilding and Bodmer, 2014). This allows determining the selectivity of the treatment for the particular type of cancer that is being studied. On this basis, in our study it was only possible to determine the SI on the hepatocellular carcinoma lines.

It can appreciate in Table 2 the SI values reached are greater than 1. That means that compounds **(2)**, **(3)** and **(3Ac)** were more selective for

Table 2. Cytotoxic activity of selected compounds isolated from *C. incisa* leaves.

Compounds[a]	IC_{50} (μg/mL)												
	HepG2	SI	Hep3B	SI	Hela	SI	PC3	SI	MCF7	SI	A549	SI	IHH
(2)	75 ± 6	1.33	73 ± 7	1.37	82 ± 8	-	75 ± 5	-	ND	-	>100	-	100
(3)	ND	-	55 ± 5	1.82	ND	-	53 ± 4	-	ND	-	ND	-	100
(3Ac)	50 ± 3	1.56	49 ± 4	1.59	63 ± 7	-	43 ± 4		-	-	87 ± 8	-	78 ± 7
(4)	>100	-	>100	-	>100	-	>100	-	>100	-	>100	-	>100
(4Ac)	>100	-	>100	-	>100	-	>100	-	>100	-	>100	-	>100
(5)	>100	-	>100	-	>100	-	>100	-	>100	-	>100	-	>100
Paclitaxel	64×10^{-3}	1.24	33×10^{-3}	2.41	4.78×10^{-3}	-	10.2×10^{-3}	-	4.27×10^{-3}	-	5.12×10^{-3}	-	79.4×10^{-3}

[a] 2,3-dihydroxypropyl tetracosanoate **(2)**; *β*-sitosterol-D-glucopyranoside **(3)**; *β*-sitosteryl *β*-D-tetraacetyl glucopyranoside **(3Ac)**; *α*-amyrin-3-O-*β*-D-glucopyranoside **(4)**; *α*-amyrin tetraacetyl 3-O-*β*-D-glucopyranoside **(4Ac)**; cerebrosides **(5)**.

tumor cells, even with their low cytotoxic effects. **(3Ac)** achieved better IC_{50} and SI values on HepG2 and Hep3B cell lines, without exceeding Paclitaxel.

4. Discussion

Several plants are used today in traditional medicine in the world, without being scientifically validated. In the course of our investigations, we previously have determined the therapeutic potential of the extracts and some isolated compounds of *C. incisa* (Nocedo-Mena et al., Unpublished results). The current study leads to the isolation and characterization of various compounds, among them, β-sitosterol-D-glucopyranoside **(3)** and α-amyrin-3-*O*-β-D-glucopyranoside **(4)**, have been studied by other authors in relation to their antibacterial and cytotoxic activities (Salama et al., 2012; Araújo et al., 2017; Nzogong et al., 2018). Previous and current findings can be able to justify the use of this plant in traditional Mexican medicine to treat certain ailments, infectious or cancerous.

Cerebrosides **(5-IV**; **5-V)** and the ceramide **(1)** isolated from this plant are sphingolipids reported for the first time. Sphingolipids and their derivatives are ubiquitous bio-active components of cells. They are structural elements in the lipid bilayer and contribute to the dynamic nature of the membrane.

Complex sphingolipids in plants are formed by a ceramide back-bone comprised of a LCB esterified to a LCFA or to a very long chain (VLCFA). Cerebrosides are glycosphingolipids consisting of a ceramide and a single sugar residue at C-1. The sugar moiety is either glucose or galactose. These amphipathic molecules, cerebrosides, have been reported to exhibit a variety of biological effects on ulcer gastritis and tumors, immune reinforcement, as well as inhibitory effect on angiogenesis in some cancers (Lee et al., 2015; Michaelson et al., 2016). Ceramides have also been tested as active metabolites. Over the past 30 years, ceramides have been found to mediate biological processes as diverse as maintaining cell membrane dynamics, fluidity, and internal transport through it. Furthermore, they play a fundamental role in the regulation of cell viability, senescence, differentiation, the cell cycle and the stress response through a series of signaling cascades (Canals et al., 2018). In addition, ceramides are associated with different pathological disorders such as cancer, liver disease, diabetes, cardiovascular disease and lung inflammation, which has sparked interest in the field of pharmaceutical development, highlighting research related to antimicrobial (Bano et al., 2019) and anticancer properties (Ryland et al., 2013; Morad et al., 2017).

Regarding to biological assays, only **(4)** and **(5)** showed antibacterial activity (MIC = 100 μg/mL) against *P. aeruginosa* resistant to carbapenems. The result for the amyrin-3-O-β-D-glucopyranoside **(4)** agrees with Vázquez et al. (2012), who reported the antimicrobial activity of pentacyclic triterpenes with MIC range of 64–1088 μg/mL against ATCC strains of *S. aureus*, *S. epidermidis*, *K. pneumoniae*, *E. coli*, *P. aeruginosa*. However, in relation to cerebrosides **(5)**, our results did not accord with those Cateni et al. (2003). In their case, the cerebrosides were inactive, exhibiting MIC >200 μg/mL against ATCC strains of *S. aureus* and *E. coli*.

As can be appreciated in Table 1, in general sense, the acetylated derivatives did not outperform their natural products in the antibacterial action. For the sterol glucoside, this result agrees with that obtained by Abreu et al. (2011), who concluded that the free hydroxyl group at position 3 could be related to the bactericidal activity of the compounds tested. The results of the low antibacterial activity of the acetylated derivatives of ceramides and cerebrosides are in accordance with those reported by Mõuts et al. (2018). In their study, these researchers refer to the importance of the functional groups C-1 (OH) and C-3 (OH) of the LCB for interlipid interaction and lateral segregation in ceramide-rich domains, this being one of the mechanisms by which ceramides modify the permeability of membranes. However, obtaining semi-synthetic derivatives is a strategy used to improve multiple characteristics of natural antibiotics, such as: improving potency and spectrum, particularly activity against resistant organisms; as well as reducing toxicity and other undesirable effects (Brown and Dawson, 2015).

Concerning the tested strains, we found that the most sensitive was PARC (MIC = 100 μg/mL), while the most resistant was MRSA (MIC >200 μg/mL). In a recently published study, the antibacterial activity of ceramides isolated from *C. incisa* against CRAB reached MIC = 50 μg/mL (Nocedo-Mena et al., 2020). All these results suggest that *C. incisa* sphingolipids are active against Gram-negative species. The fact that some phytocompounds of this plant are active in these bacteria makes them good candidates for developing novel antibacterials. Further investigations could be made to evaluate the combination of the above natural products with commercial antibacterials that currently cannot be used to treat Gram-negative infections due to poor accessibility by the cellular envelope of these bacteria. In this sense, natural products and those optimized by synthesis or semisynthesis will become the next generation of antibacterial agents (Brown and Dawson, 2015).

The findings related to the cytotoxic activity, revealed that compound **(3Ac)** exhibited the best IC_{50} values against PC3 (43 ± 4 μg/mL) and Hep3B (49 ± 4 μg/mL) cells. Previously, it has been determinate the capacity of this natural product to perturbing the cell cycle and inducing apoptotic cell death in cancer cells (Rajavel et al., 2017).

In relation to the selectivity on the hepatocellular carcinoma cell lines, the SI values reached were more significant than 1.0, which makes all assayed compounds more selective for tumor cells. This result is consistent with the work of Shen et al. (2018), who obtained good scores testing triterpenes and glycosides against a hepatocellular cancer line by induction of apoptosis. The structure-activity relationship established for these authors concluded that the hydroxyl or monosaccharide at position C-3, make the compounds show better cytotoxic activity. The selectivity obtained for Hep3B is interesting because, in this type of cancer, the p53 gene involved in apoptosis, is mutated. Several studies suggest that phytosterols disrupt the cell cycle and induce apoptosis by activating caspases 3 and 9 in cancer cells, suggesting their use for the treatment of this cancer (Maiyo et al., 2016).

In a general sense, natural products have long been explored as invaluable sources of inspiration for drug design, with particular effectiveness in cancerous and infectious diseases (Rodrigues et al., 2016). Other studies with natural products in the treatment of cancer have shown synergistic effects of the combination with chemotherapeutic agents (Zong et al., 2019).

5. Conclusions

Our study constitutes the first characterization of the ceramide 2-(2′-hydroxydecanoyl amino)-1,3,4-hexadecanotriol-8-ene **(1)**, and cerebrosides **(5-IV**, **5-V)**. At the same time, compound **(2)** and all sphingolipids obtained are reported for the first time within *Cissus*. Only α-amyrin-3-*O*-β-D-glucopyranoside **(4)** and cerebrosides mixture **(5)** exhibited activity (MIC = 100 μg/mL) against *P. aeruginosa* resistant to carbapenems. Meanwhile, β-sitosteryl β-D-tetraacetyl glucopyranoside **(3Ac)** was the most active on PC3 (IC_{50} = 43 ± 4 μg/mL) and the most selective on HepG2 and Hep3B cancer lines. The Selectivity Index reached on the hepatocellular carcinoma lines, revealed potentialities of the compounds to treat selectively this type of cancer.

This research reveals the importance of study medicinal plants from the chemical and pharmacological point of view, to contribute to the scientific knowledge, and as sources of potential drugs. The traditional use of *C. incisa* leaves in traditional Mexican medicine is justified; however, other studies would be needed to confirm the safety and efficacy of the plant. Further investigations could be made to assess the synergistic

effects of combining the above natural products with chemotherapeutic and antibacterial agents in the face of increased of these diseases.

Declarations

Author contribution statement

Deyani Nocedo-Mena: Performed the experiments; Analyzed and interpreted the data; Wrote the paper.

Verónica M. Rivas-Galindo, Patricia Navarro, Elvira Garza-González, Leticia González-Maya, María Yolanda Ríos, José Rodríguez-Rodríguez: Performed the experiments; Contributed reagents, materials, analysis tools or data.

Abraham García, Francisco G. Ávalos-Alanís: Performed the experiments; Analyzed and interpreted the data.

María del Rayo Camacho-Corona: Conceived and designed the experiments; Contributed reagents, materials, analysis tools or data; Wrote the paper.

Funding statement

María del Rayo Camacho-Corona was supported by Universidad Autónoma de Nuevo León (04-093765-FAR-11/250-FCQ-UANL).

Competing interest statement

The authors declare no conflict of interest.

Additional information

No additional information is available for this paper.

Acknowledgements

The authors acknowledge the biologist M. González Ferrara for the plant identification and the sample collection. As well as the kind collaboration of Esther Lete, Nuria Sotomayor, and Humbert González-Díaz from the Department of Organic Chemistry II, University of the Basque Country UPV/EHU, Spain.

References

Abreu, V.G.C., Takahashi, J.A., Duarte, L.P., Piló-Veloso, D., Junior, P.A.S., Alves, R.O., Romanha, A.J., Alcántara, A.F.C., 2011. Evaluation of the bactericidal and trypanocidal activities of triterpenes isolated from the leaves, stems, and flowers of *Lychnophora pinaster*. Brazilian J. Pharma 21, 615–621.

Alvarado Vázquez, M.A., Rocha Estrada, A., Moreno Limón, S., 2010. De la lechuguilla a las biopelículas vegetales: las plantas útiles de Nuevo León. Monterrey, Nuevo León, México.

Araújo, C.R., Silva, R., Silva, T., Takahashi, J., Sales-Junior, P., 2017. Constituents from stem barks of *Luehea ochrophylla* Mart and evaluation of their antiparasitic, antimicrobial, and antioxidant activities. Nat. Prod. Res. 31, 1948–1953.

Badisa, R.B., Darling-Reed, S.F., Joseph, P., Cooperwood, J.S., Latinwo, L.M., Goodman, C.B., 2009. Selective cytotoxic activities of two novel synthetic drugs on human breast carcinoma MCF-7 cells. Anticancer Res. 29, 2993–2996.

Bano, S., Faizi, S., Lubna, Fayyaz, S., Iqbal, E.Y., 2019. Isolation of ceramides from *Tagetes patula* L. yellow flowers and nematicidal activity of the fractions and pure compounds against Cyst nematode, *Heterodera zeae*. Chem. Biodivers. 16, e1900092.

Basu, A., Saito, K., Meyer, K., Ray, R.B., Friedman, S.,L., Chang, Y.-H., Ray, R., 2006. Stellate cell apoptosis by a soluble mediator from immortalized human hepatocytes. Apoptosis 11, 1391–1400.

Brown, P., Dawson, M.J., 2015. A perspective on the next generation of antibacterial agents derived by manipulation of natural products. In: Witty, D.R. (Ed.), Progress in Medicinal Chemistry. Elsevier B.V.

Canals, D., Salamone, S., Hannun, Y., 2018. Visualizing bioactive ceramides. Chem. Phys. Lipids 216, 142–151.

Cateni, F., Zilic, J., Falsone, G., Scialino, G., Banfi, E., 2003. New cerebrosides from *Euphorbia peplis* L.: antimicrobial activity evaluation. Bioorg. Med. Chem. Lett 13, 4345–4350.

Chipiti, T., Ibrahim, M.A., Singh, M., Islam, M.S., 2017. In vitro α-amylase and α-glucosidase inhibitory and cytotoxic activities of extracts from *Cissus cornifolia* Planch Parts. Pharmacogn. What Mag. 13, 329–333.

El-halawany, A.M., Osman, S.M., Abdallah, H.M., 2018. Cytotoxic constituents from Vicia monantha subsp. monantha seeds. Nat. Prod. Res. 33, 1783–1786.

Fernandes, G., Banu, J., 2012. Medicinal properties of plants from the genus *Cissus*: a review. J. Med. Plants Res. 6, 3080–3086.

Fouche, G., Ramafuthula, M., Maselela, V., Mokoena, M., Senabe, J., Leboho, T., Sakong, B.M., Adenubi, O.T., Eloff, J.N., Wellington, K.W., 2016. Acaricidal activity of the organic extracts of thirteen South African plants against *Rhipicephalus* (Boophilus) *decoloratus* (Acari: ixodidae). Vet. Parasitol. 224, 39–43.

Gezici, S., Şekeroğlu, N., 2019. Current perspectives in the application of medicinal plants against cancer: novel therapeutic agents. Anticancer. Agents Med. Chem. 19, 101–111.

Hernández-Galicia, E., Calzada, F., Roman-Ramos, R., Alarcón-Aguilar, F.J., 2007. Monoglycerides and fatty acids from *Ibervillea sonorae* root: isolation and hypoglycemic activity. Planta Med. 73, 236–240.

Inagaki, M., Isobe, R., Kawano, Y., Miyamoto, T., Komori, T., Higuchi, R., 1998. Isolation and structure of three new ceramides from the starfish *Acanthaster planci*. European J. Org. Chem. 1, 129–131.

Kang, W.Y., Li, C.Q., Ji, Z.Q., 2011. A new carbamic acid from *Dryopteris wallichiana*. Chem. Nat. Compd. 47, 91–93.

Kiplimo, J.J., Koorbanally, N.A., Chenia, H., 2011. Triterpenoids from *Vernonia auriculifera* Hiern exhibit antimicrobial activity. African J. Pharmacol. Pharm. 5, 1150–1156.

Kumar, M., Talreja, T., Jain, D., Dhuria, R.K., 2017. Comparative evaluation of *in vitro* antibacterial activity of several extracts of *Achyranthes aspera, Azolla pinnata, Cissus quadrangularis* and *Tinospora cordifolia*. International Journal of Chemical Studies 5, 154–157.

Learn2Grow, 2016. Cissus incisa. http://www.learn2grow.com/plants/cissus-incisa/. (Accessed 9 February 2020).

Lee, S.R., Jung, K., Noh, H.J., Park, Y.J., Lee, H.L., Lee, K.R., Kang, K.S., Kim, K.H., 2015. A new cerebroside from the fruiting bodies of *Hericium erinaceus* and its applicability to cancer treatment. Bioorg. Med. Chem. Lett 25, 5712–5715.

Lin, W.Y., Yen, M.H., Teng, C.M., Tsai, I.L., Chen, I.S., 2004. Cerebrosides from the rhizomes of Gynura japonica. J. Chin. Chem. Soc. 51, 1429–1434.

Lü, J.L., Duan, J.A., Tang, Y.P., Ge, Y.L., 2008. Two new ceramides from the radix of. Angelica sinensis. Journal of Chemical Research 658–661.

Maiyo, F., Moodley, R., Singh, M., 2016. Phytochemistry, cytotoxicity and apoptosis studies of β-Sitosterol-3-*O*- Glucoside and β-Amyrin from. Prunus africana. Afr. J. Tradit. Complement. Altern. Med 13, 105–112.

Mbosso, E.J.T., Ngouela, S., Nguedia, J.C.A., Penlap Bengs, V., Rohmer, M., Tsamo, E., 2008. Spathoside, a cerebroside and other antibacterial constituents of the stem bark of *Spathodea campanulata*. Nat. Prod. Res. 22, 296–304.

McCarthy, F.O., Chopra, J., Ford, A., Hogan, S.A., Kerry, J.P.B., O'Brien, N.M., Ryanb, E., Maguirea, A.R., 2005. Synthesis, isolation and characterization of β-sitosterol and β-sitosterol oxide derivatives. Org. Biomol. Chem. 3, 3059–3965.

Michaelson, L.V., Napier, J.A., Molino, D., Faure, J.D., 2016. Plant sphingolipids: their importance in cellular organization and adaption. Biochim. Biophys. Acta 1861, 1329–1335.

Morad, S.A.F., Davis, T.S., MacDougall, M.R., Tan, S.F., Feith, D.J., Desai, D.H., Amin, S.G., Kester, M., Loughran, T.P., Cabot, M.C., 2017. Role of P-glycoprotein inhibitors in ceramide-based therapeutics for treatment of cancer. Biochem. Pharmacol. 130, 21–33.

Möuts, A., Vattulainen, E., Matsufuji, T., Kinoshita, M., Matsumori, N., Slotte, J.P., 2018. On the importance of the C(1)-OH and C(3)-OH functional groups of the long-chain base of ceramide for interlipid interaction and lateral segregation into ceramide-rich domains. Langmuir 34, 15864–15870.

Ndhlovu, D.N., Masika, P.J., 2017. *In vitro* efficacy of extracts from plants used by small-holder farmers in the treatment of dermatophilosis in cattle. Afr. J. Tradit., Complementary Altern. Med. 14, 263–272.

Njinga, N.S., Sule, M.I., Pateh, U.U., Hassan, H.S., Abdullahi, S.T., Ache, R.N., 2016. Isolation and antimicrobial activity of β-sitosterol-3-O-glucoside from lannea kerstingii engl. & K. Krause (anacardiacea). Nitte Univ. J. Health Sci. 6, 4–8.

Nocedo-Mena, D., Garza-González, E., González-Ferrara, M., Camacho-Corona, M., 2020. Antibacterial activity of *Cissus incisa* extracts against multidrug- resistant bacteria. Curr. Top. Med. Chem. 20, 1–6.

Nocedo-Mena, D., Rios, M.Y., Ramírez-Cisneros, M.Á., González-Maya, L., Sánchez-Carranza, J.N., Camacho Corona, M.R., et al., 2020. Metabolomic profiling of three extracts from *Cissus incisa* leaves and its correlation with *in vitro* cytotoxic activity. Phytomedicine. Submitted for publication.

Nzogong, R.T., Ndjateu, F., Ekom, S.E., Fosso, J.M., Awouafack, M.D., Tene, M., Tane, P., Morita, H., Choudhary, M.I., Tamokou, J.D., 2018. Antimicrobial and antioxidant activities of triterpenoid and phenolic derivatives from two Cameroonian Melastomataceae plants: *Dissotis senegambiensis* and *Amphiblemma monticola*. BMC Complement. Altern. Med 18.

Peshin, T., Kar, H., 2017. Isolation and characterization of β-sitosterol-3-*O*-β-D-glucoside from the extract of the flowers of *Viola odorata*. Br. J. Pharmaceut. Res. 16, 1–8.

Rajavel, T., Mohankumar, R., Archunan, G., Ruckmani, K., Devi, K.P., 2017. Beta sitosterol and Daucosterol (phytosterols identified in *Grewia tiliaefolia*) perturbs cell cycle and induces apoptotic cell death in A549 cells. Sci. Rep. 7, 1–15.

Rodrigues, T., Reker, D., Schneider, P., Schneider, G., 2016. Counting on natural products for drug design. Nat. Chem. 8, 531–541.

Rossiter, S., Fletcher, M., Wuest, W., 2017. Natural products as platforms to overcome antibiotic resistance. Chem. Rev. 117, 12415–12474.

Ryland, L.K., Doshi, U.A., Shanmugavelandy, S.S., Fox, T.E., Aliaga, C., Broeg, K., Baab, K.T., Young, M., Khan, O., Haakenson, J.K., Jarbadan, N.R., Liao, J., Wang, H.G., Feith, D.J., Loughran, T.P., Liu, X., Kester, M., 2013. C6-ceramide nanoliposomes target the warburg effect in chronic lymphocytic leukemia. PloS One 8, 1–15.

Salama, M., Kandil, Z., Islam, W., 2012. Cytotoxic compounds from the leaves of *Gaillardia aristata* Pursh growing in Egypt. Nat. Prod. Res. 26, 2057–2062.

SEINet, 2019. Cissus trifoliate. http://swbiodiversity.org/seinet/taxa/index.php?taxon=3579. (Accessed 15 February 2020).

Shen, S., Li, W., Ouyang, M., Wang, J., 2018. Structure-activity relationship of triterpenes and derived glycosides against cancer cells and mechanism of apoptosis induction. Nat. Prod. Res. 32, 654–661.

Suffness, M., Pezzuto, J., 1990. Assays related to cancer drug discovery. In: Assays for Bioactivity Methods in Plant Biochemistry. Academic Press, London, pp. 71–133.

Sugiyama, S., Honda, M., Higuchi, R., Komori, T., 1991. Stereochemistry of the four diastereomers of ceramide and ceramide lactoside. Liebigs Ann. Chem. 1991, 349–356.

Tacconelli, E., Carrara, E., Savoldi, A., Harbarth, S., Mendelson, M., Monnet, D., 2018. Discovery, research, and development of new antibiotics: the WHO priority list of antibiotic-resistant bacteria and tuberculosis. Lancet Infect. Dis 18, 318–327.

Tapondjou, L.A., Mitaine-Offer, A.C., Sautour, M., Miyamoto, T., Lacaille-Dubois, M.A., 2005. Sphingolipids and other constituents from *Cordia platythyrsa*. Biochem. Systemat. Ecol. 33, 1293–1297.

Vázquez, L.H., Palazon, J., Navarro-Ocaña, A., 2012. The pentacyclic triterpenes α, β amyrins: a review of sources and biological activities. In: Rao, W. (Ed.), Phytochemicals - A Global Perspective of Their Role in Nutrition and Health, Toronto, pp. 487–502.

Vega-Ávila, E., Velasco-Lezama, R., Jiménez-Estrada, M., 2006. Las plantas como fuentes de compuestos antineoplásicos. Bioquimia 31, 97–111.

WHO, 2017. WHO publishes the list of bacteria for which new antibiotics are urgently needed. http://www.who.int/mediacentre/news/releases/2017/bacteria-antibiotics-needed. (Accessed 3 January 2020).

Wilding, J.L., Bodmer, W.F., 2014. Cancer cell lines for drug discovery and development. Can. Res. 74, 2377–2384.

Zgoda, J.R., Porter, J.R., 2001. A convenient microdilution method for screening natural products against bacteria and fungi. Pharmaceut. Biol. 39, 221–225.

Zhang, W.K., Xu, J., Zhang, X., Yao, X., Ye, W.C., 2007. Sphingolipids with neuritogenic activity from *Euphorbia sororia*. Chem. Phys. Lipids 148, 77–83.

Zong, L., Chenga, G., Liu, S., Pi, Z., Liu, Z., Song, F., 2019. Reversal of multidrug resistance in breast cancer cells by a combination of ursolic acid with doxorubicin. J. Pharmaceut. Biomed. Anal. 165, 268–275.